Characterisation of shallow aquifers by 2D high-resolution seismic data analysis

M. Giustiniani, F. Accaino, E. Del Negro, S. Picotti and U. Tinivella

Istituto Nazionale di Oceanografia e di Geofisica Sperimentale, Trieste, Italy

(Received: August 12, 2007; accepted: September 30, 2007)

ABSTRACT We present the results obtained processing high-resolution seismic data acquired along the resurgence line located in the Friuli-Venezia Giulia plain (NE Italy), in order to characterize an important multilayered aquifer. This system is made up of an unconfined layer and, at increasing depths, of several confined aquifers of variable thickness and hydraulic permeability, mainly consisting of sandy/gravelly material. The main targets of this study are two shallow aquifers located at a depth of about 30 m and 180 m, respectively. The velocity model obtained reveals lateral velocity variations with a maximum value of 600 m/s. The higher velocities could be associated with layers constituting confined aquifers. Pre-stack depth migration using the above velocity model gives a clear picture of the multilayered aquifer, highlighting lateral changes in reflectivity.

1. Introduction

Population growth and industrial development have enormously increased water consumption to such a point that fresh water is becoming one of the most important natural resources. For this reason, many nations all over the world have exacted long term sustainable policies for the protection and public use of water. An example of such policies is the European Water Framework Directive 2000/60/CE, through which the European Union aims to achieve a "good ecological status" for surface water and groundwater.

The application of seismic reflection methods to shallow hydrogeological problems was not technically or economically viable until the 1980s. In the last 20 years, the seismic reflection technique has been adapted for many hydrogeological purposes, with different degrees of success (Steeples and Miller, 1990; Bachrach and Nur, 1998; Bradford, 1998; Cardimona *et al*., 1998; Whiteley *et al*., 1998).

Our research objective is the acquisition, processing and interpretation of high-resolution seismic data in order to characterize the geological structures in the shallow subsoil. The proposed methodology has been tested in an area located along the resurgence line of the Friuli-Venezia Giulia plain (north-eastern Italy). This area includes a sedimentary sequence, settling between Mesozoic and Quaternary. After an extensional tectonic phase during the Mesozoic, a Cenozoic compressional phase, connected to Dinaric and Alpine structures, caused the deposition of turbiditic sediments (Nicolich *et al*., 2004). At the test site, the Miocenic sediments, underlying Plio-quaternary layers, are directly in contact with Mesozoic carbonates. The test site was suitable for our experiment because of the presence of highly permeable sedimentary layers that host an important aquifer system. In that area, however, intensive agricultural and industrial activities, as

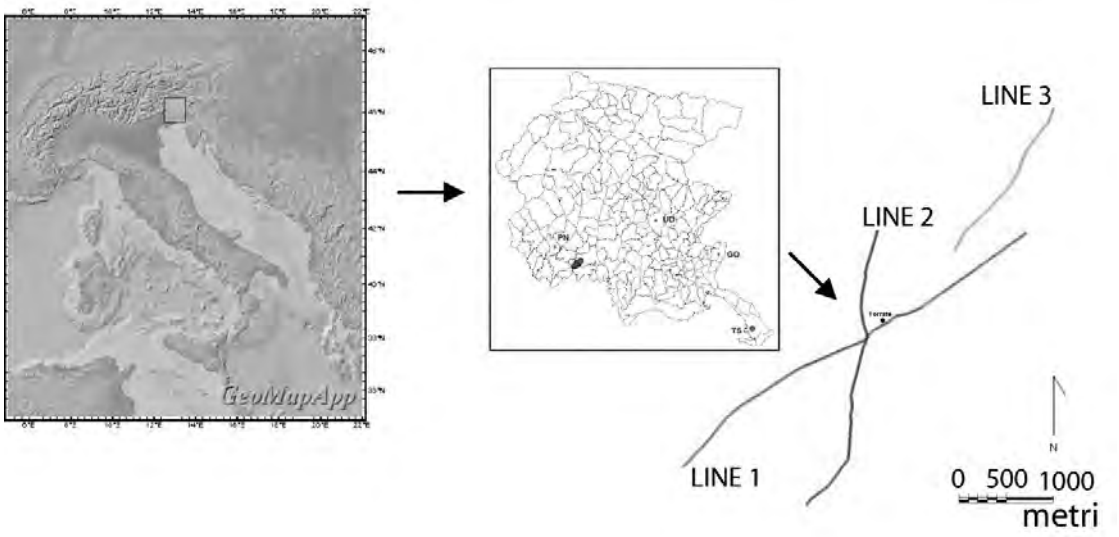

Fig. 1 - Location map of the 2D seismic lines.

well as intense urbanization, may cause pollution hazards.

During the winter of 2005, three seismic lines were acquired to determine a preliminary subsurface geometry and analyze the seismic response of the aquifers (Fig. 1). This preliminary acquisition was planned to optimize a later 4D survey. We will focus our attention on the results obtained from the two longer lines (profiles 1 and 2 in Fig. 1).

The processing, described in the following paragraphs, was focused on enhancing the signal-to-noise ratio and increasing the vertical resolution by adopting the 'true-amplitude' (Yilmaz, 2001) in order to perform Amplitude Versus Offset analysis (AVO) (Tinivella *et al*., 2007).

Finally, we used the interval velocity fields obtained from the travel-time tomographic inversion (Vesnaver *et al*., 1999) to perform a 2D pre-stack depth migration of the processed seismic data, in order to build a realistic depth section of the investigated area.

2. Preliminary modelling

We built an initial 3D geophysical model by using the stratigraphy of several catchment wells of the "Basso Livenza" Aqueduct. Thickness, P- and S-wave velocity, density and quality factors of both P and S waves are reported in Table 1. Some seismic sections of the Italian "CROsta Profonda" (CROP) Project were used too [Scrocca *et al*. (2003), Nicolich *et al*. (2004), among others]. This model included water-saturated gravel layers alternated by clay impermeable layers (see Fig. 2 and Table 1). In the following step, synthetic seismograms were created by using commercial software (Fig. 2).

We carried out a numerical wave-simulation of two shots in the seismic model using a P-wave source for the first and an S-wave source for the second. The offset ranges from 0 to 4 km and the source is a dilatation force located at the surface, whose time-history is a Ricker wavelet with

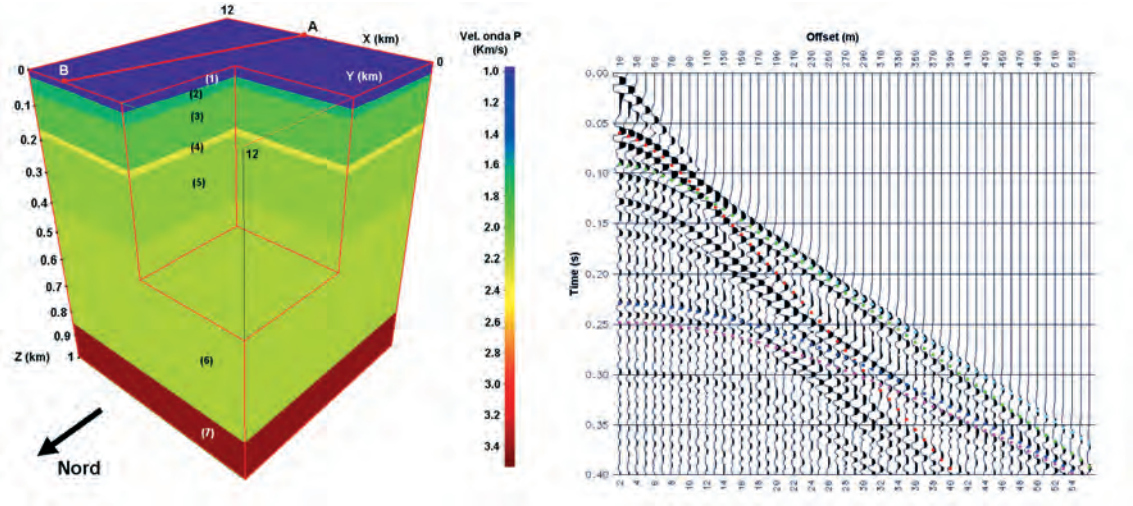

Fig. 2 - Left: 3D seismic model of the aquifer, whose seismic parameters are shown in Table 1. The seismic simulation was carried out along line AB, which fits the 2D seismic survey analyzed here (Line 2). Right: The synthetic seismogram of the first shot recorded at the surface: the vertical particle-velocity component is represented, and the dominant frequency is 80 Hz. The events of interest are the reflections of the second layer (red and green) and the fourth layer (blue and purple), and the refraction of the second layer (sky-blue).

Table 1 - Seismic properties of the aquifer model shown in Fig. 2: compressional-wave (P) and shear-wave (S) velocities, density, and quality factors (Bourbié *et al*., 1987; Prasad and Meissner, 1992; Schön, 1996). The values in brackets refer to the overpressure condition (see text). The seismic parameters of layer 6 (velocity and density) are linearly interpolated.

Layer	Medium	Mean thickness	V_P (m/s)	V_S (m/s)	r (kg/m^3)	Q_P	Q_S
1	Clay+gravel	27	1000	300	1700	20	20
2	Saturated gravel	55	1600 (1564)	450 (427)	1900 (1890)	40 (40)	40 (40)
3	Clay	178	1800	600	2000	30	30
4	Saturated gravel	200	2200 (2142)	800 (767)	2100 (2080)	50 (50)	50 (50)
5	Clay	400	2000	700	2200	40	40
6	Gravel+sand+clay (top)	850	1800	600	1900	60	60
	Gravel+sand+clay (bottom)		2500	1000	2300	60	60
7	Carbonatic basement		3500	1900	2800	100	100

a dominant frequency of 80 Hz. The purpose of the modelling was to optimize the seismic acquisition configuration in order to have the appropriate characteristics for a reliable tomographic inversion, i.e. a sufficient resolution and coverage, in particular to detect the shallower aquifer.

Moreover, the synthetic seismograms allow us to better distinguish the reflection and refraction events in the real data. Fig. 2 shows that the refracted wave from the second aquifer is not evident, while the refracted event related to the first aquifer is hardly detectable, with a crossover offset of about 400 m. Moreover, a far offset of at least 1 km is necessary to have information about the refracted wave of the deeper layer (400 m).

3. Seismic data acquisition

The seismic acquisition was focused on the two main aquifers that are at a depth of about 30 m and 180 m, respectively. Preliminary field tests were also performed in order to define the best sweep of the vibroseis and to analyze the strong ground-roll and the environmental noise. Tests were carried out using different sweep lengths and frequency windows. Using frequencies above 150 Hz, the data resolution did not increase and the amplitude spectra of the shallower reflections had a maximum frequency of about 140 Hz. The shot tests confirmed the acquisition parameters defined by the preliminary modelling.

During the winter of 2005, three 2D seismic lines were acquired with a total length of 10 km. The survey map (Fig. 1) shows that the data acquisition was strongly influenced by the presence of human urbanization. We used a Summit acquisition system, with a minimum of 260 active channels, and a vibroseis as seismic source. The receiver and shot intervals were 5 m and 10 m respectively, giving a common depth point every 2.5 m. The signal sweep of 12 s in length and a frequency range of 10-150 Hz were used to provide 3 s-length records with a time sampling of 1 ms after cross-correlation of recorded data with the pilot trace. The chosen pattern configuration was asymmetrical with a maximum offset of 300 m and 1000 m respectively, to the left and to the right of the shot.

4. Processing of seismic data

The quality of the raw data was satisfactory, despite the ground-roll. The reflections of interest are evident from 0.03 s to about 1.1 s, while the refractions are not always detectable because of velocity inversions caused by the alternation of permeable and impermeable layers. The seismic lines were located near the main road, so the effects of running vehicles were evident, in particular on the data of Line 1.

The processing focused on enhancing the signal-to-noise ratio and increasing the vertical resolution by adopting the ‘true-amplitude’ approach, in order to preserve the relative true amplitudes of the signal. Firstly, we deleted the traces showing a persistent level of noise. Then, we applied a band-pass filter 20-160 Hz to eliminate the low frequencies related to the ground-roll and a 50 Hz notch filter to suppress the power-line noise. After a spherical divergence correction, the data were deconvolved using a 200 ms length predictive deconvolution operator with a gap of 8 ms and a white noise level of 1%. Fig. 3 shows that the deconvolution greatly

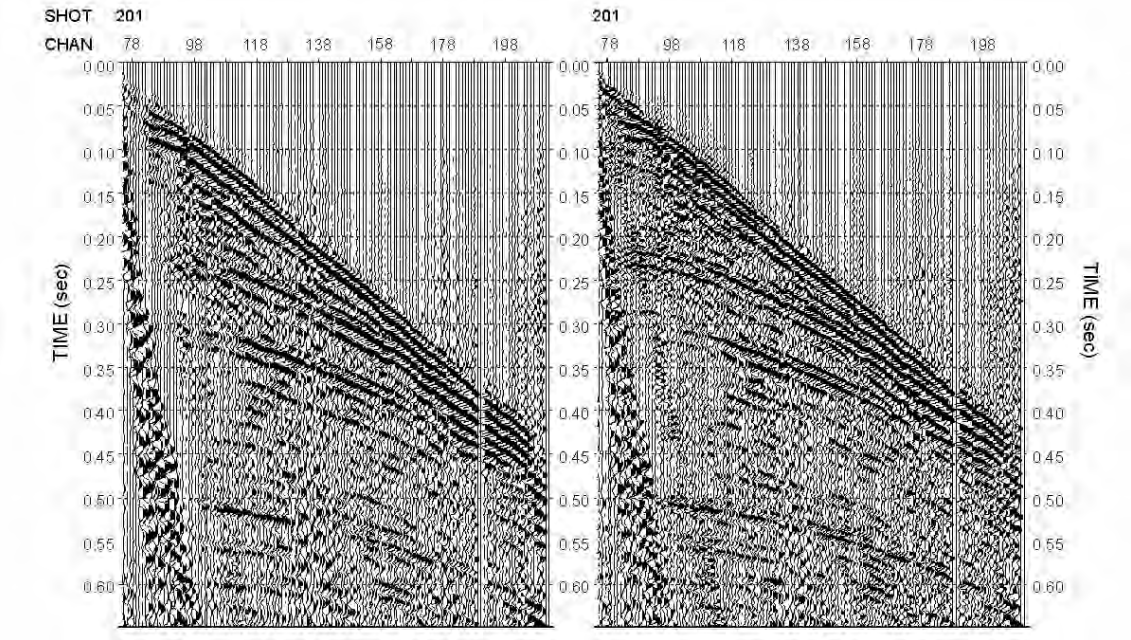

Fig. 3 - Field record of line 1 before (left) and after predictive deconvolution (right). Both reverberations and ground roll were attenuated, allowing the identification of the previously hidden signals.

improved the vertical resolution of the data.

A trimmed, mean dynamic dip filter was applied to the shot domain in order to attenuate the ground-roll (Holcombe and Wojslaw, 1992; Yilmaz, 2001) and so facilitate the picking of the reflected events used for the tomographic inversion. Within the studied area, the presence of soft plough, harder untilled land and roads causes strong shallow lateral velocity variations. Thus, we performed a surface-consistent residual static correction using the tomographic velocity field that allows an accurate result because of its reliability. The tomographic technique, in fact, is based on the ray theory, so it is more reliable than the stacking velocity analysis methods. Then, the tomographic velocity fields, converted from interval to RMS velocity, were used to stack the data, after the application of an external mute function to remove the direct arrivals. We were very careful not to modify the amplitude spectrum. A time-variant filter and F-X deconvolution were applied to the post-stack data to increase the signal-to-noise ratio and the lateral continuity of the signal.

The final stacked sections are shown in perspective in Fig. 4. Note the good correlations between the main reflectors at the intersection of Lines 1 and 2.

5. Velocity analysis

We reconstructed the aquifer depth structures by performing a tomographic inversion of reflected arrivals. Fig. 5 shows a few picked reflections in a common shot gather, where we can notice a good lateral coherency of the signal. The adopted tomographic method (Vesnaver *et al*.,

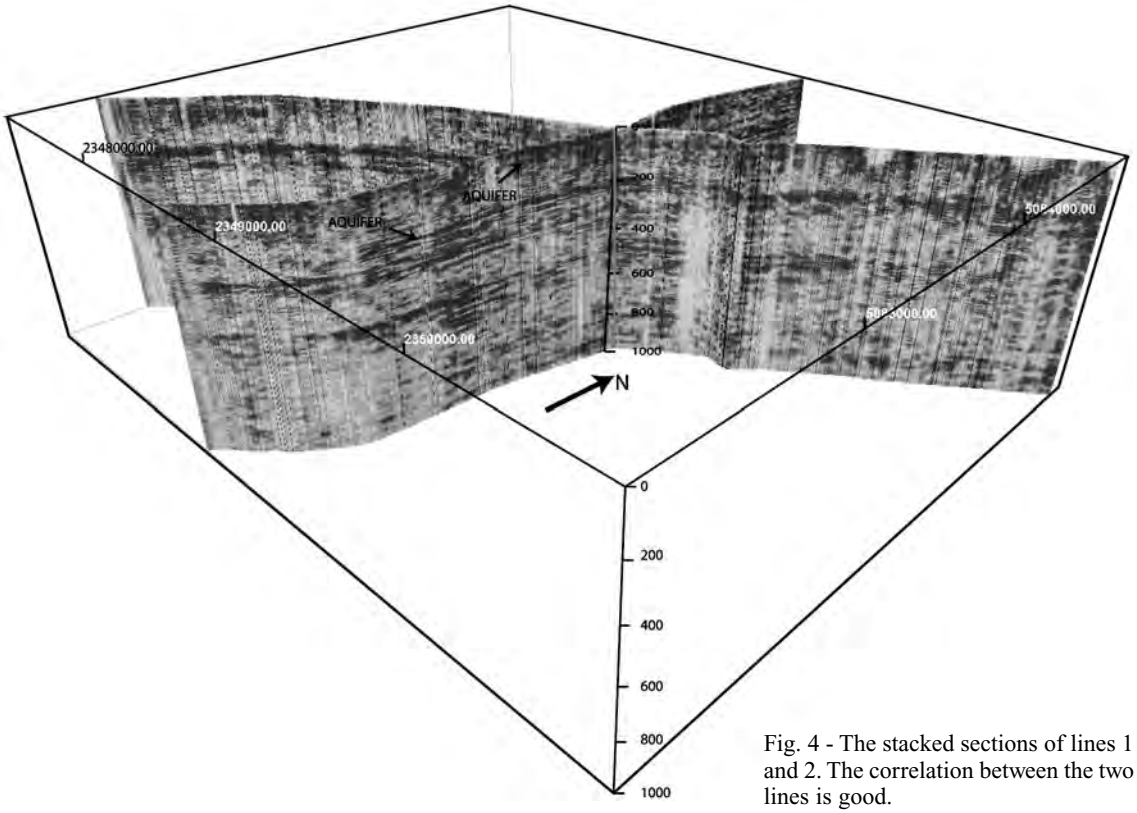

Fig. 4 - The stacked sections of lines 1 and 2. The correlation between the two lines is good.

1999) is based on the simultaneous iterative reconstruction procedure algorithm (Van der Sluis and Van der Vorst, 1987; Stewart, 1991) and the minimum-time ray tracing (Böhm and Vesnaver, 1999). We estimated velocity field and reflector structure in sequence, from the upper to the deeper horizon. The model is blocky, with voxels where the velocity is assumed to be vertically constant between the chosen reflectors. The base and top of the voxels define the reflecting and refracting interfaces that may be curved and dipping.

For each horizon we used an iterative procedure (Fig. 5), starting from a constant velocity within the layer and horizontally flat interface. Our initial model is shown in Fig. 2 and Table 1. In each iteration, we first inverted the picked travel times of reflected events and updated the velocity model. Then, we estimated the new interfaces following the principle of minimum dispersion of the reflected points. The travel time residual associated to each reflected event was converted in depth by using the velocity field updated in the first step of any iteration. Within each single iteration, we could optimise the grid by using an adaptive grid updating (Fig. 5). At the end of the inversion we computed the traveltimes and, in order to evaluate the reliability of the tomographic model, we applied the chi-squared test to the picked traveltime fit (Zelt and Smith, 1992).

The inversion proceeded by simultaneous adjustment of the velocity field and the depth of the interfaces to improve the picked traveltimes fit. The overall fit improved about ten times during

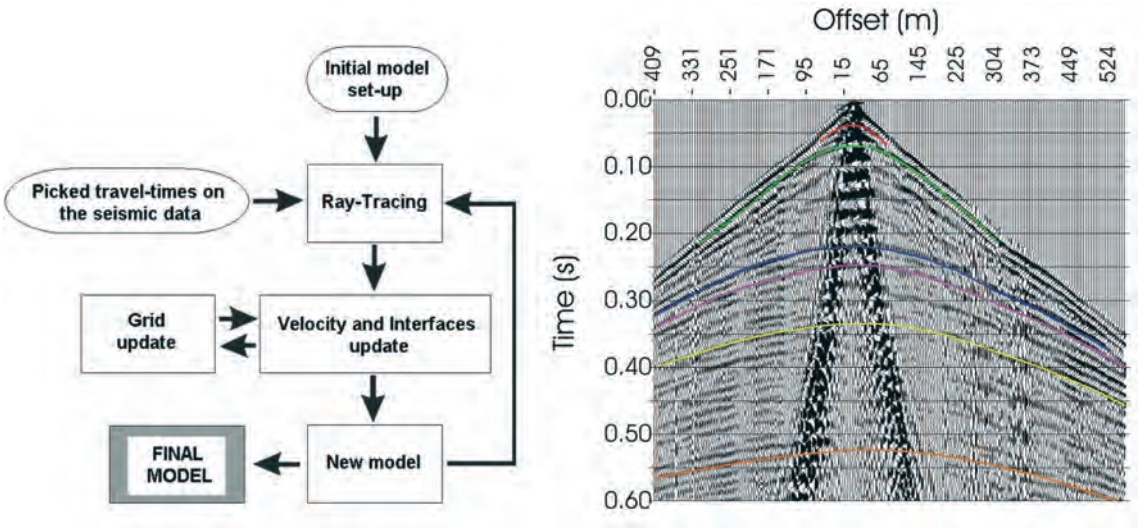

Fig. 5 - Left: A flowchart of the travel-time tomography algorithm adopted. Right: Example of picking of a real shot gather, where the amplitude is related to the vertical particle-velocity component. In this picture the picking of the following horizons is represented: the PP reflections from the first aquifer (red and green), the PP reflections from the second aquifer (blue and purple) and the PP reflections from the deeper interfaces (yellow and orange).

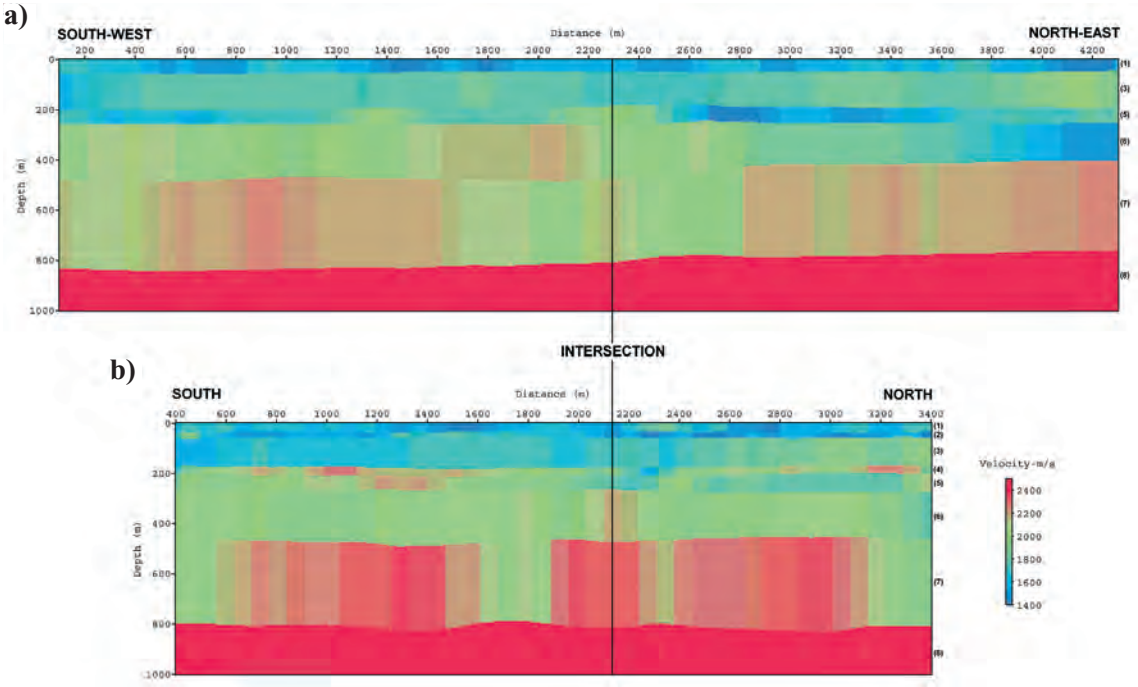

Fig. 6 - Tomographic velocity (P waves) model respectively for Line 1 (a) and Line 2 (b).

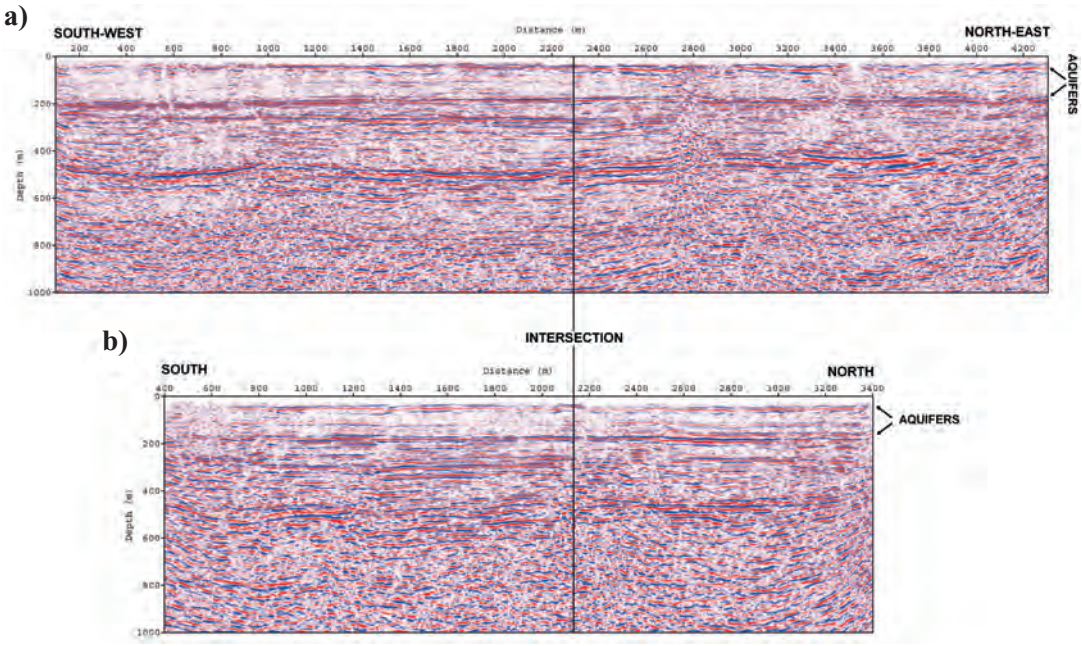

Fig. 7 - Prestack depth migration respectively for Line 1 (a) and Line 2 (b).

the inversion, from a misfit about 20 chi-squared for the initial model to 1.9 for the final model. Figs. 6 and 7 show the tomographic P-wave velocity model and the pre-stack migrated depth sections of the two 2D seismic, respectively. In the inversion of Line 2, we also tried to recover the thickness of the two aquifers (layers 2 and 4). Considering a medium error of ± 6 ms in the picking, the maximum error in the evaluation of the velocity inside the two aquifers is of about ±15 m/s.

The two shallow aquifers are nearly flat and show noticeable lateral velocity variations with a maximum excursion of about 600 m/s, whereas the structures of the deeper reflectors are more irregular. The tomographic model (Fig. 6) confirms the presence of a velocity inversion between the fourth (second aquifer) and fifth layer and shows the correlation between high velocities and sediments constituting aquifers, as indicated from the well stratigraphy (Table 1). Comparing the migrated sections and the velocity models of the two lines at their intersection, we found a good correlation both for the depth of the reflectors and the layer velocities. The comparison of the two velocity models (Fig. 6) shows velocity differences of about 100 m/s in the deeper layers. These differences are related to the increase of the velocity error that could be at estimated at about 5% for our inversion algorithm (Tinivella *et al*., 2002) and to the decrease of the fold because the line intersection was close to the road.

6. Discussion and conclusions

The results obtained show that seismic data can characterize some lithological property and

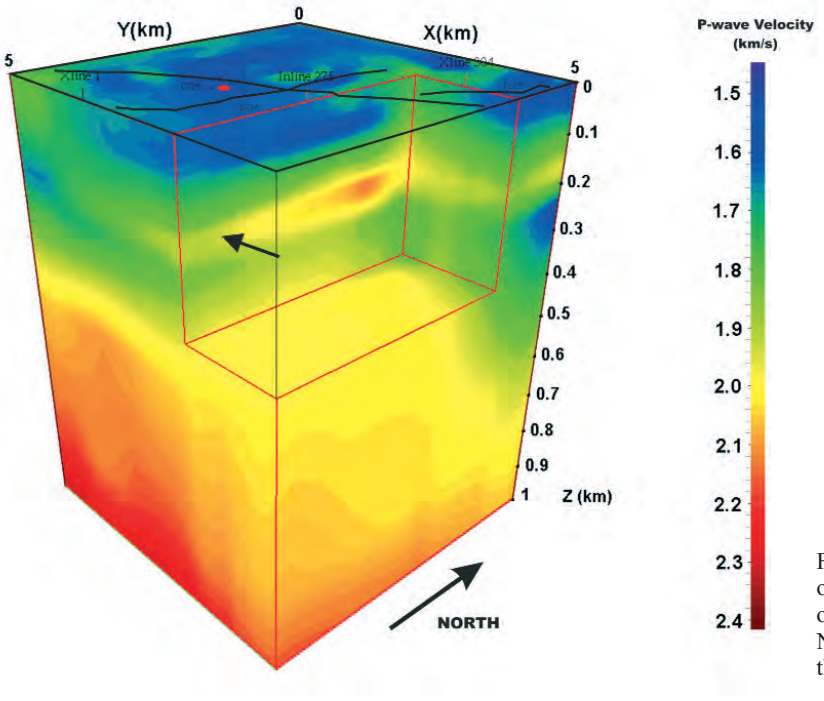

Fig. 8 - 3D velocity model, obtained from the interpolation of three 2D velocity fields. Note the second main aquifer thins south words.

the geometry of a multilayered aquifer system. Numerical wave simulations of synthetic seismograms, based on the seismic parameters obtained from well information, allowed the optimisation of the acquisition configuration. The acquired seismic allowed the travel-time inversion of reflected P arrivals, with the purpose of imaging the aquifers' structure. The tomographic velocity models (Fig. 6) and the migrated sections (Fig. 7) show that the shallowest structures are more regular than the deeper ones.

Two, main deeper reflectors are evident at a depth of about 500 m related to a deep aquifer and another one at about 800 m, which could be interpreted as a Miocenic layer. At the intersection of the two seismic lines, both the velocity models and the migrated sections fit well.

Finally, the 3D velocity model obtained from the interpolation of three 2D velocity fields (Fig. 8) points out that the second aquifer has strong lateral variation. The thinning in the southern part, as indicated by the black arrow, is in accordance with the hydrogeological data. A catchment well, drilled about 20 years ago, showed the absence of the deeper aquifer in this area (Enrico Marin, personal communication).

Acknowledgments. We acknowledge the European Community that has supported this project (LIFE Project Number - LIFE04 ENV/IT/000500). We wish to thank the Acquedotto Basso Livenza, and in particular Enrico Marin, for the logistical support and all the information provided (hydrogeological data and the stratigraphies of the catchment wells). Thanks to Serguei Bouriak for his technical support in the use of the RadExPro Plus (Deco Geophysical) software.

REFERENCES

Bachrach R. and Nur A.; 1998: *High-resolution shallow-seismic experiments in sand, Part I: Water table, fluid flow, and saturation.* Geophysics, **63**, 1225-1233.

Böhm G. and Vesnaver A.L.; 1999: *In quest of the grid.* Geophysics, **64**, 1116-1125.

Bourbié T., Coussy O. and Zinzner B.; 1987: *Acoustics of porous media.* Gulf Publishing, Houston, Texas, 56 pp.

Bradford J.H.; 1998: *Characterizing shallow aquifers with seismic reflection, part II – Prestack depth migration and field examples.* Geophysics, **67**, 98-109.

Cardimona S.J., Clement W.P. and Kadinsky-Cade K.; 1998: *Seismic reflection and ground-penetrating radar imaging of a shallow aquifer*. Geophysics, **63**, 1310–1317.

Holcombe H.T. and Wojslaw R.S.; 1992: *Spatially weighted trim stacking: a technique for pre-stack noise suppression.* In: Proceedings Society of Exploration Geophysicists, 62nd SEG Annual Meeting, New Orleans, USA, pp. 1157-1160.

Nicolich R., Della Vedova B., Giustiniani M. and Fantoni R.; 2004: *Carta del sottosuolo della Pianura Friulana.* Litografia Cartografica, Firenze.

Prasad A. and Meissner G.; 1992: *Attenuation mechanism in sands: laboratory versus theoretical (Biot) data.* Geophysics, **57**, 710-719.

Schön S.; 1996: *Physical properties of rocks-Fundamentals and principles of petrophysics.* Handbook of Geophysical Exploration: Seismic Exploration, vol. 18, Pergamon, Oxford, UK; Tarrytown, N. Y., 583 pp.

Scrocca D., Doglioni C., Innocenti F., Manetti P., Mazzotti A., Bertelli L., Burbi L. and D'Offizi S. (eds); 2003: *CROP ATLAS - Seismic reflection profiles of the Italian crust.* Memorie Descrittive Carta Geologica d'Italia 62, 194 pp.

Steeples D.W. and Miller R.D.; 1990: *Seismic-reflection methods applied to engineering, environmental, and ground-water problems.* In: Ward S. (ed), Geotechnical and Environmental Geophysics, 1, Review and Tutorial, Investigations in Geophysics No. 5, Soc. Expl. Geophys., pp. 1-30.

Stewart R.R.; 1991: *Exploration seismic tomography: fundamentals.* Soc. of Explor. Geophys., Course Note Series, Vol. 3, 190 pp.

Tinivella U., Accaino F. and Camerlenghi A.; 2002: *Gas hydrate and free gas distribution from inversion of seismic data on the South Shetland margin (Antarctica).* Marine Geophysical Research, **23**, 109-123.

Tinivella U., Accaino F., Giustiniani M. and Picotti S.; 2009: *Petro-physical characterization of shallow aquifers by using AVO and theoretical approaches.* Boll. Geof. Teor. Appl., **50**, 59-69.

Van der Sluis A. and Van der Vorst H.A.; 1987: *Numerical solutions of large, sparse linear systems arising from tomographic problems.* In Nolet G. (ed), Seismic tomography, D. Reidel Pub., Dordrecht, Holland, pp. 49–84.

Vesnaver A., Böhm G., Madrussani G., Petersen S. and Rossi G.; 1999: *Tomographic imaging by reflected and refracted arrivals at the North Sea.* Geophysics, **64**, 1852-1862.

Whiteley R.J., Hunter J.A., Pullan S. E. and Nutalaya P.; 1998: "*Optimum offset" seismic reflection mapping of shallow aquifers near Bangkok, Thailand.* Geophysics, **63**, 1385-1394.

Yilmaz O.; 2001: *Seismic data analysis: processing, inversion and interpretation of seismic data.* Society of Exploration Geophysicists, Tulsa, Oklahoma, 2027 pp.

Zelt C.A. and Smith R.B.; 1992: *Seismic traveltime inversion for 2-D crustal velocity structure.* Geophysical Journal International, **108**, 16-34.

Corresponding author: Michela Giustiniani
Dipartimento Geofisica della Litosfera
Istituto Nazionale Oceanografia e di Geofisica Sperimentale
Borgo Grotta Gigante 42/c, Sgonico (Trieste), Italy
phone: +39 040 2140259; fax: +39 040 327307; e-mail: mgiustiniani@inogs.it